Published in final edited form as:
Am J Physiol Gastrointest Liver Physiol. 2004 February ; 286(2): G333–G339. doi:10.1152/ajpgi.00289.2003.

Norepinephrine effects on identified neurons of the rat dorsal motor nucleus of the vagus

Isabel Martinez-Peña y Valenzuela[1], **Richard C. Rogers**[2], **Gerlinda E. Hermann**[2], and **R. Alberto Travagli**[1,3]

[1]Department of Internal Medicine-Gastroenterology, University of Michigan, Ann Arbor, Michigan 48109

[2]Laboratory of Autonomic Neuroscience, Pennington Biomedical Research Center, Baton Rouge, Louisiana 70808

[3]Department of Physiology, University of Michigan, Ann Arbor, Michigan 48109

Abstract

The dorsal motor nucleus of the vagus (DMV) receives more noradrenergic terminals than any other medullary nucleus; few studies, however, have examined the effects of norepinephrine (NE) on DMV neurons. Using whole cell recordings in thin slices, we determined the effects of NE on identified gastric-projecting DMV neurons. Twenty-five percent of DMV neurons were unresponsive to NE, whereas the remaining 75% responded to NE with either an excitation (49%), an inhibition (26%), or an inhibition followed by an excitation (4%). Antrum/pylorus- and corpus-projecting neurons responded to NE with a similar percentage of excitatory (49 and 59%, respectively) and inhibitory (20% for both groups) responses. A lower percentage of excitatory (37%) and a higher percentage of inhibitory (36%) responses were, however, observed in fundus-projecting neurons. In all groups, pretreatment with prazosin or phenylephrine antagonized or mimicked the NE-induced excitation, respectively. Pretreatment with yohimbine or UK-14304 antagonized or mimicked the NE-induced inhibition, respectively. These data suggest that NE depolarization is mediated by α_1-adrenoceptors, whereas NE hyperpolarization is mediated by α_2-adrenoceptors. In 16 neurons depolarized by NE, amplitude of the action potential afterhyperpolarization (AHP) and its kinetics of decay (τ) were significantly reduced vs. control. No differences were found on the amplitude and τ of AHP in neurons hyperpolarized by NE. Using immunohistochemical techniques, we found that the distribution of tyrosine hydroxylase fibers within the DMV was significantly different within the mediolateral extent of DMV; however, distribution of cells responding to NE did not show a specific pattern of localization.

Keywords

brain stem; electrophysiology; gastrointestinal-receptive relaxation

Sensory information from the gastrointestinal (GI) tract is received and integrated by neurons in the nucleus of the solitary tract (NTS), in which it is modulated and transferred to neurons in the dorsal motor nucleus of the vagus (DMV) (1,2,21). DMV neurons then provide efferent outflow to the GI tract (28,29). Catecholamine-containing neurons originating in the locus coeruleus as well as A_2 noradrenergic neurons within the NTS

Address for reprint requests and other correspondence: R. A. Travagli, Univ. of Michigan, 6520 MSRB 1, 1150 West Medical Center Dr., Ann Arbor, MI 48109 (Travagli@umich.edu).

project to nuclei within the brain stem (9,14,25). Within the brain stem, the DMV receives more projections from noradrenergic fiber terminals than any of the other medullary nuclei (20). Sumal et al. (24) showed that the A_2 noradrenergic area receives direct excitatory synaptic inputs from sensory vagal afferents, whereas Fukuda et al. (9) demonstrated that electrical stimulation of the A_2 area induces profound catecholaminergic effects on unidentified DMV neurons. Finally, Miyamoto et al. (17) showed that local brain stem application of norepinephrine (NE) increases cervical vagal efferent discharge via an effect on α-adrenoceptors, and more recently, we (5) have demonstrated that endogenous catecholamines modulate the glutamatergic pathway from the subnucleus commissuralis of the NTS to the DMV via presynaptic α_2-adrenoceptors. These data suggest that catecholamines might modulate vagovagal reflexes regulating GI functions. Indeed, we have shown that repetitive esophageal distension activates central NTS neurons (21), that the majority of these neurons are tyrosine hydroxylase (TH)-immunoreactive (-IR), and that the gastric relaxation induced by esophageal distension could be antagonized by both α_1- and α_2-adrenoceptors (23). Despite the mounting evidence involving catecholaminergic projections in the control of vagovagal reflexes, however, no systematic study of the effects of NE has been conducted on gastric-projecting DMV neurons.

In the present study, we aimed to determine at the cellular level the effects of NE on identified gastric-projecting DMV neurons.

MATERIALS AND METHODS

Retrograde tracing

GI-projecting DMV neurons were labeled as described previously (6). Briefly, 10- to 12-day-old Sprague-Dawley rat pups (Charles River Laboratories, Wilmington, MA) of either sex were anesthetized (indicated by abolition of the foot pinch withdrawal reflex) with a 6% solution of 2-bromo-2-chloro-1,1,1-trifluoroethane (halothane) with air (400–600 ml/min). Anesthesia was maintained by placing the head of the rat in a custom-made anesthetic chamber through which the halothane mixture was perfused. A laparotomy was performed, during which crystals of the retrograde tracer 1,1′-dioctadecyl-3,3,3′,3′-tetramethylindocarbocyanine perchlorate (DiI; Molecular Probes, Eugene, OR) were applied to the serosal surface of either the stomach fundus, corpus, or antrum/pylorus, and the application site was embedded in a fast-hardening epoxy resin that was allowed to dry for several minutes before the entire surgical area was washed with warm saline (6). The wound was closed with 5-0 suture, and the animal was allowed to recover for 10–15 days. Animal care and experimental procedures were performed with the approval of the Animal Care and Utilization Committee of the University of Michigan.

Electrophysiology

Brain stems were removed as described previously (6,26). Briefly, the rats were anesthetized with halothane. When a deep level of anesthesia was induced, the rat was killed by severing the major blood vessels in the chest. The brain stem was then removed and placed in oxygenated Krebs solution at 4°C (see *Solution composition*). The site of DiI labeling in the stomach was confirmed by visual inspection of the organ. The brain stem was used only from those animals in which the glue covering the site of DiI application was still in place at the time of the experiment. With the use of a vibratome, six to eight coronal sections (200-μm thick) containing the dorsal vagal complex (DVC) were cut and stored in oxygenated Krebs solution at 30°C for at least 1 h before use. A single slice was transferred to a custom-made perfusion chamber (volume 500 μl) and kept in place by using a nylon mesh. The chamber was maintained at 35 ± 1°C by perfusion with warmed, oxygenated Krebs solution at a rate of 2.5–3.0 ml/min.

Before electrophysiological recording, gastric-projecting DMV neurons were identified by using a Nikon E600-FN microscope equipped with epifluorescent filters suitable for visualizing DiI. Once the identity of a labeled neuron was confirmed, whole cell recordings were made under bright-field illumination by using DIC (Nomarski) optics.

Whole cell recordings were made with patch pipettes (3–8 MΩ resistance) filled with a potassium gluconate solution (see *Solution composition*) by using an Axoclamp 2B single-electrode voltage-clamp amplifier (Axon Instruments, Union City, CA). Recordings were made only from neurons unequivocally labeled with DiI. Data were sampled every 100 μs and filtered at 2 kHz, digitized via a Digidata 1200C interface (Axon Instruments) and acquired, stored, and analyzed on an IBM PC utilizing pClamp 8 software (Axon Instruments). Recordings were accepted only if the series resistance was <15 MΩ. In addition, the action potential evoked after injection of depolarizing current must have had an amplitude of at least 60 mV and the membrane potential had to return to the baseline value after the action potential afterhyperpolarization (AHP). Drugs were made fresh immediately before use and were applied to the bath via a series of manually operated valves.

Concentration-response curves were constructed from fundus-, corpus-, and antrum/pylorus-projecting neurons in which at least three concentrations of NE were tested. For measurements of the NE-induced depolarization or hyperpolarization, neurons were hyperpolarized to −65 mV via injection of direct current; for measurements of the effects of NE on the spontaneous action potential discharge rate, neurons were held at their resting potential ($I = 0$). When tested on spontaneously active DMV neurons, the NE-induced variation in firing rate was measured as the number of action potentials counted during the 20 s preceding the administration of the drug and during the 20 s of maximal firing rate variation after drug superfusion. Cells were defined as responders if NE (10 μM) induced a change in the membrane potential of at least 3 mV or a 20% variation in the action potential discharge rate.

Morphological reconstructions

At the end of the electrophysiological recordings, before removal of the pipette, Neurobiotin (2.5% wt/vol) was injected into the DMV (0.4 nA, 600 ms on/1,200 ms off for 10 min). After injection of Neurobiotin, the pipette was retrieved from the cell, which was allowed to seal for 10–20 min before overnight fixation at 4°C in Zamboni's fixative (see *Solution composition*). The diaminobenzidine-horseradish peroxidase technique used to develop the Neurobiotin stain and the protocol used for neuronal reconstruction have been described previously (6).

Immunohistochemistry

Five rats were injected with Fluoro-Gold (20 μg·ml saline^{-1}·rat^{-1} ip) (Fluorochrome, Englewood, CO) 3 days before brain stem removal to label preganglionic neurons innervating the subdiaphragmatic viscera, allowing delineation of the boundaries of the DMV (11,19,32). Rats were anesthetized deeply (abolition of foot pinch withdrawal reflex) with halothane and perfused with 200 ml saline followed by 200 ml Zamboni's fixative.

After extraction, brain stems were fixed in Zamboni's fixative overnight, rinsed with PBS containing Triton X-100 (PBS-TX) and stored in PBS-TX overnight at 4°C. The brain stem was then placed in a 2.5% sucrose-in-PBS solution before coronal sections of 40-μm thickness were cut by using a cryostat. Every third slice was mounted onto gelatin-coated coverslips. The portion of the DMV located caudal to the obex was defined as the caudal DMV and the portion of DMV located rostral to the anterior tip of the area postrema as the

rostral DMV. The area comprising the extension of the area postrema was defined as the intermediate DMV.

Slices were rinsed with fresh PBS-TX-BSA solution and incubated at 37°C for 2 h with the primary antibody (mouse-α-TH; 1:500 dilution in PBS-TX containing 0.1% BSA). Slices were rinsed with PBS-TX-BSA and incubated again at 37°C for 30 min with secondary antibody (goat-α-mouse FITC; Sigma, St. Louis, MO) 1:100 dilution in PBS containing 0.1% BSA. Specimens were again rinsed with PBS-TX-BSA solution before being allowed to air dry and were mounted with Fluoromount-G (Southern Biotechnology Associated, Birmingham, AL). Control experiments were carried out to ensure that the antibody labeling was selective, namely *1*) incubation of primary or secondary antibodies only and *2*) reaction of primary antibody with inappropriate secondary antibody. All tests proved negative, indicating that the secondary antibodies were selective for their primary antibodies and that the antibodies themselves exhibited neither nonspecific binding nor excessive autofluorescence.

Optical density measurements

Tissue sections were examined and photographed with a Nikon E400 microscope equipped with epifluorescent filters for FITC and UV, SPOT camera, and software (Diagnostic Instruments, Sterling Heights, MI). The settings of the acquisition parameters were kept constant throughout the experiments. The optical density measurements of TH-IR within the DMV were analyzed by using Image J software (developed at the National Institutes of Health and available from the internet at http://rsb.info.nih.gov/ij). Background subtraction was conducted on each specimen by measuring the optical density of an area within the visual field that did not contain TH-IR somata, usually in the NTS area 100–200 μm dorsal to the DMV. Optical density measurements were calculated by subtracting the background measurement from the DMV area analyzed and are expressed in arbitrary units of fluorescence. In each group (caudal, intermediate, and rostral DMV), a minimum of 10 slices from each rat was averaged.

Statistical analysis

Results are expressed as means ± SE. Inter-group comparisons were analyzed with one-way ANOVA followed by the conservative Bonferroni test for individual post hoc comparisons, Student's paired *t*-test, or χ^2 test. Significance was defined as $P < 0.05$.

Drugs and chemicals

All drugs were purchased from Sigma (St. Louis, MO); stock solutions were freshly prepared and diluted to the final concentration in Krebs solution just before use. Permount was purchased from Fisher Scientific (Pittsburgh, PA), DiI was purchased from Molecular Probes (Eugene, OR), and Neurobiotin was purchased from Vector Labs (Burlingame, CA).

Solution composition

Krebs solution was (in mM) 126 NaCl, 25 $NaHCO_3$, 2.5 KCl, 1.2 $MgCl_2$, 2.4 $CaCl_2$, 1.2 NaH_2PO_4, and 11 dextrose, maintained at pH 7.4 by bubbling with 95% O_2-5% CO_2. Intracellular solution was (in mM) 128 potassium gluconate, 10 KCl, 0.3 $CaCl_2$, 1 $MgCl_2$, 10 HEPES, 1 EGTA, 2 ATP, and 0.25 GTP, adjusted to pH 7.35 with KOH. Zamboni's fixative was 1.6% (wt/vol) paraformaldehyde, 19 mM KH_2PO_4, and 100 mM $Na_2HPO_4 \cdot 7H_2O$ in 240 ml saturated picric acid-1,600 ml H_2O, adjusted to pH 7.4 with HCl. PBS-TX was (in mM) 115 NaCl, 75 $Na_2HPO_4 \cdot 7H_2O$, 7.5 KH_2PO_4, and 0.15% Triton X-100. Avidin D-horseradish peroxidase solution was 0.05% diaminobenzidine in PBS containing 0.5% gelatin supplemented with 0.025% $CoCl_2$ and 0.02% $NiNH_4SO_4$.

RESULTS

Whole cell patch-clamp studies were conducted on 228 identified gastric-projecting neurons (80 fundus-, 83 corpus-, and 65 antrum/pylorus-projecting neurons). All of the DMV neurons were spontaneously firing action potentials at 0.91 ± 0.08 spikes per second (n = 40). There were no differences in the firing rate between neurons that responded to NE with an increase in firing rate (0.86 ± 0.08 spikes/s; n = 31) and neurons that responded to NE with a decrease in firing rate (1.09 ± 0.24 spikes/s; n = 9; $P > 0.05$).

Analysis of the effects of NE on identified DMV neurons

Seventy-five percent of neurons (i.e., 170 of 228) responded to NE (1–100 μM) in a concentration-dependent manner. Response to NE was either an excitation (111 of 228, i.e., 49% of total or 65% of responsive neurons), an inhibition (59 of 228, i.e., 26% of total or 35% of responsive neurons), or an inhibition followed by an excitation (10 of 228, i.e., 4% of total or 6% of responsive neurons. These neurons have been included in the group defined as inhibited by NE). The remaining 58 (i.e., 25%) neurons did not respond to NE.

Interestingly, a similar proportion of antrum/pylorus- and corpus-projecting neurons were excited (49 and 59% of the total neurons, respectively) or inhibited by NE (20% of the total neurons for both groups). A lower percentage of fundus-projecting neurons, however, was excited (37% of the total neurons), and a larger percentage of neurons was inhibited by NE (36% of the total neurons, $P < 0.05$ vs. corpus- or antrum/pylorus-projecting neurons). Results are summarized in Table 1.

In all gastric-projecting groups, the threshold for the response to NE was ~1 μM and maximum current (I_{MAX}) was obtained at 100 μM; the data have thus been pooled.

To ascertain whether the NE-induced membrane effects were due to a direct effect of NE on DMV neurons, we compared the amplitude of the NE-induced membrane depolarization in the absence and presence of the synaptic transmission blocker TTX (1 μM). In seven neurons, NE (30 μM) induced a 7.1 ± 1.05-mV depolarization that recovered to baseline on washout. After 10 min of perfusion with TTX, reapplication of NE in the presence of TTX induced a 5.4 ± 0.95-mV depolarization (i.e., 78 ± 12% of control, $P > 0.05$ vs. NE alone). Similarly, in five other neurons, NE induced a 11.4 ± 1.3-mV hyperpolarization that recovered to baseline on washout. After 10 min of perfusion with TTX, reapplication of NE in the presence of TTX induced a 8.8 ± 1.3-mV hyperpolarization (i.e., 81 ± 16% of control, $P > 0.05$ vs. NE alone; data not shown).

In eight cells in which NE (30 μM) had an excitatory effect, 10-min pretreatment with the selective α_1-adrenoceptor antagonist prazosin (100 nM), which per se did not affect the basal firing rate (0.91 ± 0.17 and 0.88 ± 0.19 spikes/s in control and in prazosin, respectively; $P > 0.05$), antagonized the NE-induced increase in action potential firing rate from 380 ± 81% of control in NE alone to 98 ± 12% of control in prazosin + NE ($P < 0.05$ vs. NE alone). Similarly, in another group of neurons, pretreatment with prazosin (100 nM) attenuated the NE-induced depolarization from 9.1 ± 1.5 mV in control to 2 ± 0.5 mV after prazosin (n = 7; $P < 0.05$; Fig. 1). The NE-mediated depolarization was mimicked by perfusion with the selective α_1-adrenoceptor agonist phenylephrine (10 μM) that induced a depolarization of 4.7 ± 0.6 mV (n = 12).

In four neurons in which NE (30 μM) decreased the discharge rate to 2.8 ± 2.8% of control, 10-min pretreatment with the selective α_2-adrenoceptor antagonist yohimbine (10 μM), which per se did not affect the basal firing rate (0.81 ± 0.13 and 0.97 ± 0.09 spikes/s in control and in yohimbine, respectively; $P > 0.05$), restored the firing rate to 123 ± 16% of

control ($P < 0.05$ vs. NE alone). Similarly, in three different neurons in which NE (30 μM) induced a hyperpolarization, a 10-min pretreatment with yohimbine (10 μM) attenuated the NE-induced hyperpolarization from 9.6 ± 4 mV in NE to 2 ± 3 mV in NE + yohimbine ($P < 0.05$ vs. NE alone; Fig. 2). In four cells in which NE induced a hyperpolarization, perfusion with the selective α_2-adrenoceptor agonist UK-14304 (1 μM) also induced a hyperpolarization of 4 ± 1.4 mV.

To further support the selective activation of α_1-adrenoceptor and α_2-adrenoceptor in the excitatory and inhibitory effects of NE, respectively, we conducted the following experiments. In four neurons in which NE (100 μM) induced a depolarization, a 10-min pretreatment with yohimbine (10 μM) did not attenuate the NE-induced depolarization, which was 10.5 ± 0.5 mV in NE and 9.3 ± 1.5 mV in NE + yohimbine ($P > 0.05$ vs. NE alone, data not shown). Likewise, in three neurons in which NE (30 μM) induced a hyperpolarization, 10-min pretreatment with prazosin (100 nM) did not attenuate the NE-induced hyperpolarization, which was 6.4 ± 1.4 mV in NE and 6.0 ± 1.1 mV in NE + prazosin ($P > 0.05$ vs. NE alone, data not shown).

In an effort to investigate the possible mechanism of action, we tested the effects of NE (30 μM) on the shape of the action potential on neurons depolarized by NE. Cells were clamped at −55 mV by injection of direct current and then injected with a 10-ms-long pulse of depolarizing current sufficient to evoke a single action potential at its offset. In control conditions, the amplitude of the AHP was 16.6 ± 0.71 mV ($n = 13$). After NE (30 μM) perfusion, current was injected to return the membrane potential to baseline values. In the presence of NE, the amplitude of the action potential AHP was reduced to 14.6 ± 0.7 mV ($P < 0.05$ vs. control). Similarly, the AHP kinetic of decay (τ) was 69 ± 9 ms in control and 55 ± 7 ms in the presence of NE ($n = 13$, $P < 0.05$ vs. control; Fig. 3). Conversely, in neurons in which application of NE (30 μM) hyperpolarized the DMV membrane, the AHP and its τ were unaltered by NE (16.4 ± 1 mV and 66 ± 16 ms and 15.3 ± 1 mV and 54 ± 10 ms in control and NE, respectively; $n = 7$; $P > 0.05$ vs. control; Fig. 3).

Analysis of the location of TH-positive neurons

Distribution of TH-IR within the DMV was analyzed by using optical density measurements. Compact neuronal organization and the presence of TH-IR-positive somata prevented a compartmentalized analysis of the caudal portion of the DMV. In fact, the optical density of TH-IR yielded similar values throughout the caudal DMV (20 ± 2 arbitrary units, $n = 5$). Conversely, in both the intermediate and rostral portions of the DMV, areas of different optical density could be distinguished throughout the rostrocaudal extent of the DMV. An area of low optical density (14 ± 1.5 and 10.4 ± 2.2 arbitrary units in the intermediate and rostral DMV, respectively) was present in the central portion of the DMV; an area of high optical density (22.7 ± 2 and 20.6 ± 1.1 arbitrary units in the intermediate and rostral DMV, respectively) was present close to the NTS, hypoglossal nucleus, and central canal (Fig. 4).

A schematic representation of the DMV was then drawn in which we divided the nucleus according to the high- and low-optical-density areas; the localization of the DMV cells in relation to their electrophysiological responses to NE (i.e., excitation, inhibition, or not responsive) was then superimposed on the schematic. We found no apparent relationship between the optical density and a particular response to NE (Fig. 5).

DISCUSSION

The present study provides evidence that *1*) NE induces a membrane depolarization, hyperpolarization, or biphasic response in subsets of DMV neurons; *2*) fundus-projecting

neurons are less likely to have an excitatory response and more likely to have an inhibitory response to NE than corpus- or A/P-projecting neurons; *3*) NE-induced depolarization is mediated by adrenoceptors and is likely due to a decrease in the AHP, whereas hyperpolarization is mediated by adrenoceptors; and *4*) within the DMV boundaries there are areas of lower TH-IR fiber density but no apparent correlation between TH-IR low-density areas and response of DMV neurons to NE.

The following evidence supports our data. Perfusion with NE induced a direct membrane response in the vast majority of DMV neurons. The most common response, observed in ~60% of the responsive neurons, consisted of a concentration-dependent excitation. A large subgroup of DMV neurons, ~35% of the responsive ones, was hyperpolarized by perfusion with NE, whereas only a limited fraction of the responsive neurons, ~5% of the total, responded to NE with an initial hyperpolarization followed by a depolarization. Interestingly, we observed that DMV neurons projecting to either the antrum/pylorus or the corpus had a similar incidence of neurons responding to NE with either excitatory or inhibitory responses. Fundus-projecting neurons, however, had a significantly lower percentage of excitatory responses and a higher percentage of inhibitory responses compared with neurons projecting to antrum/pylorus or corpus. Our data confirm and extend the previous observation reported by Fukuda et al. (9), who described similar percentages of NE-responsive neurons.

It is interesting to note that the concentration-response curve of the NE-induced decrease in firing rate shifted to the left relative to that of the NE-induced membrane hyperpolarization. We take this shifted concentration response curve as an indication of the major sensitivity of DMV neurons to inhibitory synaptic inputs utilizing catecholamines and, in general, other inhibitory neurotransmitters.

With the use of agonists and antagonists selective for subtypes of α-adrenoceptors, we demonstrated that the excitatory response to NE is mediated by interaction with α_1-adrenoceptors and that the inhibitory response to NE is mediated by interaction with postsynaptic α_2-adrenoceptors. Our data confirm the conclusions reached by Fukuda et al. (9), which suggested α_1- and α_2-adrenoceptors as the receptors responsible for the actions of NE on unidentified DMV neurons.

Our data suggest that, at least in part, the excitatory effects of NE are due to a reduction of the amplitude and kinetics of decay of the action potential AHP. An excitatory effect on vagal motor neurons determined by a reduction of the AHP is similar to our recent reports on the effects of corticotropin-releasing factor and thyrotropin-releasing hormone in DMV neurons (15,27) and similar to other reports of the effects of NE in cardiopulmonary vagal motor neurons (18) or in hypothalamic neurons (30). Our data also suggest that the calcium-dependent potassium current underlying the AHP might contribute to the resting membrane potential. Interestingly, although Fukuda et al. (9) suggested that the NE-mediated hyperpolarization of DMV neurons was mediated by an increase in a potassium-sensitive current, we did not observe any significant variation of the action potential AHP in cells that were inhibited by NE. It is reasonable to assume that, given that the complement of membrane currents present in DMV neurons is dependent on the peripheral projection area (6) and that Fukuda et al. (9) conducted their recordings on unidentified DMV neurons, the cells from which Fukuda et al. (9) recorded projected to areas other than the gastric areas targeted in the present investigation.

DMV is a brain stem area that contains a very pronounced network of TH-IR fiber terminals (3,14,20) and is possibly the nucleus with the highest density of TH-IR-positive fibers within the brain stem (20). Although we cannot say with certainty that all of the TH-IR-

positive terminals are catecholaminergic, relatively recent data would suggest a 1:1 distribution of TH and dopamine-β-hydroxylase (31), thus suggesting that NE is the neurotransmitter involved in these synaptic contacts. Optical density measurements we report in the present study clearly demonstrate that within the DMV, distribution of the TH-IR-positive fibers is nonhomogeneous. In fact, a careful examination of the figures presented in the work by previous investigators (3,14) clearly shows areas of lesser density of TH-IR-positive fibers located along the same mediolateral extension reported here. Given that these areas represent approximately one-fourth of the DMV, and a similar percentage of DMV neurons did not respond to NE, we investigated whether the NE-nonresponsive neurons were localized in the areas that showed a low density of TH-IR-positive fibers. Our data, however, show that this is not the case. In fact, the type of response, or lack thereof, to NE did not correlate to any particular location of the DMV neurons.

Physiological significance

Several authors (9,14,17,24) have put forward the idea of a possible role of catecholamines in the modulation of brain stem vagal circuits. The majority of local synaptic inputs onto DMV neurons arises from the adjacent NTS, which contains the A2 catecholaminergic group (14). With the noticeable exception of the esophageal-mediated gastric relaxation (21,28), the vast majority of vagovagal reflexes induce a powerful inhibition of the DMV firing rate via activation of inhibitory NTS neurons, which then inhibit DMV vagal output (4,7,8,10,[13],16,22,28,29). An inhibitory effect on gastric tone and motility, however, can also be attained by stimulation of DMV neurons forming inhibitory nonadrenergic, noncholinergic pathways (12,28). Indeed, we have shown that repetitive esophageal stimulation induces gastric inhibition via activation of neurons in the subnucleus centralis of the NTS (cNTS) and both excitation and inhibition of DMV neurons (21). More recently, we (23) have shown that the vast majority of the cNTS neurons are TH-IR positive and that administration on the surface of the fourth ventricle of both α_1- and α_2-antagonists significantly attenuates the esophageal distension-induced gastric relaxation. We would therefore like to suggest that part of gastric relaxation induced by esophageal distension is mediated by NE acting on α_1- and α_2-adrenoceptors present on the membrane of gastric-projecting DMV neurons and that part of the excitatory response observed following NE perfusion is due to an effect on the action potential AHP.

Acknowledgments

We thank Dr. Kirsteen N. Browning for comments on earlier versions of the manuscript. We acknowledge the support and encouragement of Cesare M. Travagli, Richard F. Rogers, Lois M. Rogers, and John Hermann.

GRANTS

This work is supported by National Institute of Diabetes and Digestive and Kidney Diseases Grants DK-55530 and DK-56373.

REFERENCES

1. Altschuler SM, Bao X, Bieger D, Hopkins DA, Miselis RR. Viscerotopic representation of the upper alimentary tract in the rat: sensory ganglia and nuclei of the solitary and spinal trigeminal tracts. J Comp Neurol. 1989; 283:248–268. [PubMed: 2738198]
2. Altschuler SM, Ferenci DA, Lynn RB, Miselis RR. Representation of the cecum in the lateral dorsal motor nucleus of the vagus nerve and commissural subnucleus of the nucleus tractus solitarii in rat. J Comp Neurol. 1991; 304:261–274. [PubMed: 1707898]
3. Armstrong DM, Manley L, Haycock JW, Hersh LB. Co-localization of choline acetyltransferase and tyrosine hydroxylase within neurons of the dorsal motor nucleus of the vagus. J Chem Neuroanat. 1990; 3:133–140. [PubMed: 1971179]

4. Azpiroz F, Malagelada JR. Perception and reflex relaxation of the stomach in response to gut distention. Gastroenterology. 1990; 98:1193–1198. [PubMed: 2323512]
5. Bertolino M, Vicini S, Gillis RA, Travagli RA. Presynaptic alpha-2 adrenoceptors inhibit excitatory synaptic transmission in rat brain stem. Am J Physiol Gastrointest Liver Physiol. 1997; 272:G654–G661.
6. Browning KN, Renehan WE, Travagli RA. Electrophysiological and morphological heterogeneity of rat dorsal vagal neurones which project to specific areas of the gastrointestinal tract. J Physiol. 1999; 517:521–532. [PubMed: 10332099]
7. Chen CH, Rogers RC. Central inhibitory action of peptide YY on gastric motility in rats. Am J Physiol Regul Integr Comp Physiol. 1995; 269:R787–R792.
8. Fogel R, Zhang X, Renehan WE. Relationships between the morphology and function of gastric and intestinal distention-sensitive neurons in the dorsal motor nucleus of the vagus. J Comp Neurol. 1996; 364:78–91. [PubMed: 8789277]
9. Fukuda A, Minami T, Nabekura J, Oomura Y. The effects of noradrenaline on neurones in the rat dorsal motor nucleus of the vagus, in vitro. J Physiol. 1987; 393:213–231. [PubMed: 2895810]
10. Garnier L, Mei N, Melone J. Further data on the inhibitory enterogastric reflex triggered by intestinal osmotic changes in cats. J Auton Nerv Syst. 1986; 16:171–180. [PubMed: 3745774]
11. Guo JJ, Browning KN, Rogers RC, Travagli RA. Catecholaminergic neurons in rat dorsal motor nucleus of vagus project selectively to gastric corpus. Am J Physiol Gastrointest Liver Physiol. 2001; 280:G361–G367. [PubMed: 11171618]
12. Hornby PJ. Receptors and Transmission in the Brain-Gut Axis. II. Excitatory amino acid receptors in the brain-gut axis. Am J Physiol Gastrointest Liver Physiol. 2001; 280:G1055–G1060. [PubMed: 11352796]
13. Jean A. Brainstem control of swallowing: neuronal network and cellular mechanisms. Physiol Rev. 2001; 81:929–969. [PubMed: 11274347]
14. Kalia M, Fuxe K, Goldstein M. Rat medulla oblongata. II. Dopaminergic, noradrenergic (A1 and A2) and adrenergic neurons, nerve fibers, and presumptive terminal processes. J Comp Neurol. 1985; 233:308–332. [PubMed: 2858497]
15. Lewis MW, Hermann GE, Rogers RC, Travagli RA. In vitro and in vivo analysis of the effects of corticotropin releasing factor on rat dorsal vagal complex. J Physiol. 2002; 543:135–146. [PubMed: 12181286]
16. McCann MJ, Rogers RC. Impact of antral mechanoreceptor activation on the vago-vagal reflex in the rat: functional zonation of responses. J Physiol. 1992; 453:401–411. [PubMed: 1464835]
17. Miyamoto JK, Ide CH, Okubo T, Kurosawa E, Maruyama E, Fujita Y. Adrenergic nerves in the hypothalamo-bulbar pathway of the vagal nerve. J Physiol Soc Japan. 1986; 48:225.
18. Nishimura Y, Muramatsu M, Asahara T, Tanaka T, Yamamoto T. Electrophysiological properties and their modulation by norepinephrine in the ambiguus neurons of the guinea pig. Brain Research. 1995; 702:213–222. [PubMed: 8846079]
19. Powley TL, Fox EA, Berthoud HR. Retrograde tracer technique for assessment of selective and total subdiaphragmatic vagotomies. Am J Physiol Regul Integr Comp Physiol. 1987; 253:R361–R370.
20. Rea MA, Aprison MH, Felten DL. Catecholamines and serotonin in the caudal medulla of the rat: combined neurochemical-histofluorescence study. Brain Res Bull. 1982; 9:227–236. [PubMed: 7172028]
21. Rogers RC, Hermann GE, Travagli RA. Brainstem pathways responsible for oesophageal control of gastric motility and tone in the rat. J Physiol. 1999; 514:369–383. [PubMed: 9852320]
22. Rogers RC, McTigue DM, Hermann GE. Vagovagal reflex control of digestion: afferent modulation by neural and “endoneurocrine” factors. Am J Physiol Gastrointest Liver Physiol. 1995; 268:G1–G10.
23. Rogers RC, Travagli RA, Hermann GE. Noradrenergic neurons in the rat solitary nucleus participate in the esophageal-gastric relaxation reflex. Am J Physiol Regul Integr Comp Physiol. 2003; 285:R479–R489. [PubMed: 12714355]

24. Sumal KK, Blessing WW, Joh TH, Reis DJ, Pickel VM. Synaptic interaction of vagal afferents and catecholaminergic neurons in the rat nucleus tractus solitarius. Brain Res. 1983; 277:31–40. [PubMed: 6139145]
25. Ter Horst GJ, Toes GJ, Van Willigen JD. Locus coeruleus projections to the dorsal motor vagus nucleus in the rat. Neuroscience. 1991; 45:153–160. [PubMed: 1684412]
26. Travagli RA, Gillis RA, Rossiter CD, Vicini S. Glutamate and GABA-mediated synaptic currents in neurons of the rat dorsal motor nucleus of the vagus. Am J Physiol Gastrointest Liver Physiol. 1991; 260:G531–G536.
27. Travagli RA, Gillis RA, Vicini S. Effects of thyrotropin-releasing hormone on neurons in rat dorsal motor nucleus of the vagus, in vitro. Am J Physiol Gastrointest Liver Physiol. 1992; 263:G508–G517.
28. Travagli RA, Hermann GE, Browning KN, Rogers RC. Musings on the Wanderer: What's New in Our Understanding of Vago-Vagal Reflexes? III. Activity-dependent plasticity in vago-vagal reflexes controlling the stomach. Am J Physiol Gastrointest Liver Physiol. 2003; 284:G180–G187. [PubMed: 12529266]
29. Travagli RA, Rogers RC. Receptors and Transmission in the Brain-Gut Axis: Potential For Novel Therapies. V. Fast and slow extrinsic modulation of dorsal vagal complex circuits. Am J Physiol Gastrointest Liver Physiol. 2001; 281:G595–G601. [PubMed: 11518671]
30. Wagner EJ, Ronnekleiv OK, Kelly MJ. The noradrenergic inhibition of an apamin-sensitive, small-conductance Ca^{2+}-activated K^{+} channel in hypothalamic γ-aminobutyric acid neurons: pharmacology, estrogen sensitivity, and relevance to the control of the reproductive axis. J Pharmacol Exp Ther. 2001; 299:21–30. [PubMed: 11561059]
31. Willing AE, Berthoud HR. Gastric-distention-induced c-fos expression in catecholaminergic neurons of rat dorsal vagal complex. Am J Physiol Regul Integr Comp Physiol. 1997; 272:R59–R67.
32. Zheng ZL, Rogers RC, Travagli RA. Selective gastric projections of nitric oxide synthase-containing vagal brainstem neurons. Neuroscience. 1999; 90:685–694. [PubMed: 10215170]

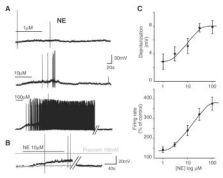

Fig. 1.

A: representative traces from the same neuron showing that perfusion with norepinephrine (NE) induces a reversible, concentration-dependent increase in firing rate. *B*: pretreatment with the α_1-antagonist prazosin attenuates the NE-induced depolarization. *Black trace*, NE alone; *gray trace*, NE + prazosin. Traces are from a neuron different from the one depicted in *A*. In both *A* and *B*, parallel oblique bars indicate a 5-min interruption of the recordings. Holding potential, −60 mV. *C*: concentration response curve for the NE-induced depolarization (*top*; n = 7–30 cells for each data point) and firing rate (*bottom*; n = 15–27 cells for each data point).

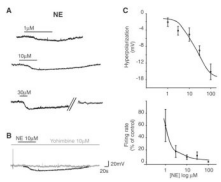

Fig. 2.

A: representative traces from the same neuron showing that perfusion with NE induces a reversible, concentration-dependent membrane hyperpolarization. Parallel oblique bars indicate a 5-min interruption of the recordings. Holding potential −60 mV. *B*: in the same neuron depicted in *A*, pretreatment with the α_2-antagonist yohimbine attenuates the NE-induced hyperpolarization. *C*: concentration response curve for the NE-induced hyperpolarization (*top*; n = 10–18 cells for each data point) and firing rate (*bottom*; n = 5–11 cells for each data point).

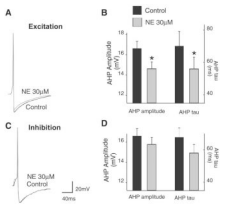

Fig. 3.

Representative traces show a single action potential before and after superfusion with 30 μM NE in two different neurons depolarized (*A*) or hyperpolarized (*C*) by NE. Summary of data illustrating the NE-induced effect on after hyperpolarization (AHP) relative to the control AHP is shown. *B*: data from neurons depolarized by NE ($n = 13$ neurons). *D*: data from neurons hyperpolarized by NE ($n = 7$ neurons). $^*P < 0.05$ vs. control. To evoke single action potentials, neurons were maintained at −60 mV by constant current injection before passing a short (10-ms) depolarizing current pulse of sufficient intensity to evoke an action potential at the offset of the pulse. During perfusion with NE, the neuronal membrane was current clamped to baseline value before an action potential was evoked.

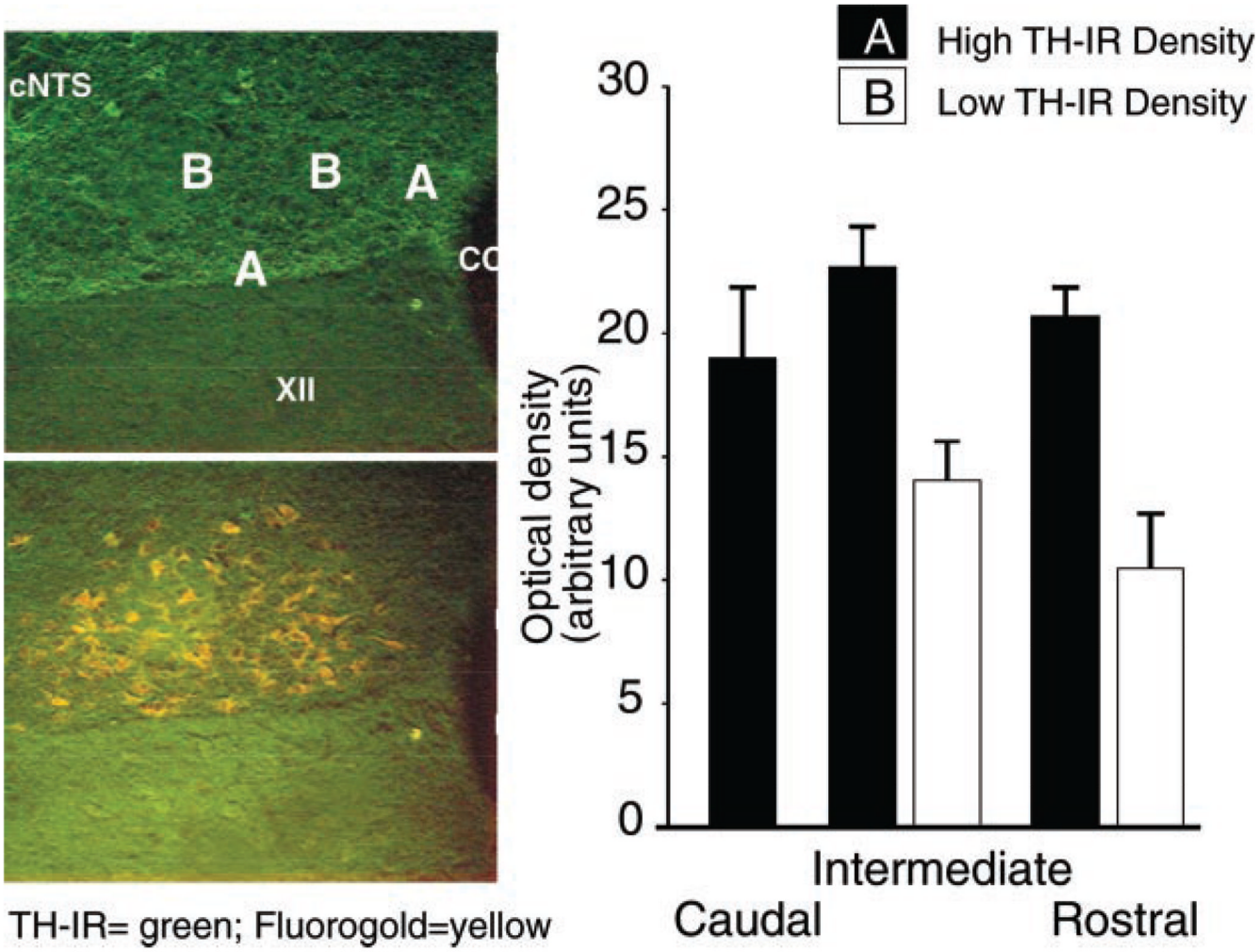

Fig. 4.

Left: representative micrograph of the intermediate portion of the dorsal motor nucleus of the vagus (DMV; the boundaries of which are delineated by the Fluoro-Gold labeling, *bottom*) showing areas of higher (A) and lower (B) density of tyrosine hydroxylase-positive immunoreactive fibers (TH-IR). XII, nucleus of hypoglossus; cNTS, subnucleus centralis of the nucleus of the solitary tract. *Right*: summary of the optical density measures (in arbitrary units) in the caudal, intermediate, and rostral portions of the DMV. *$P < 0.05$.

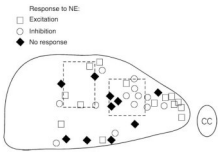

Fig. 5.

Schematic representation of the intermediate portion of the DMV. At the end of the electrophysiological recording, DMV neurons were filled with Neurobiotin to ascertain their relative localization within the DMV. Dotted rectangles schematically represent the areas in which the optical density of TH-IR was significantly lower. CC, central canal.

Table 1

Summary of responses to 10 μM norepinephrine

	n	Excitation	Inhibition	Not Responsive
Fundus	80	37*	36*	26
Corpus	83	59	20	20
Antrum/pylorus	65	49	20	31

Values are percent of total neurons.

* $P < 0.05$ vs. corpus or antrum/pylorus.